Efficient Phasor Estimation under Steady State and Dynamic Conditions

Jalal Khodaparast
Dep. of Electric Power Engineering
NTNU, Trondheim, Norway
jalal.khodaparast@ntnu.no

Olav Bjarte Fosso
Dep. of Electric Power Engineering
NTNU, Trondheim, Norway
olav.fosso@ntnu.no

Marta Molinas
Dep. of Engineering Cybernetics
NTNU, Trondheim, Norway
marta.molinas@ntnu.no

***Abstract*—Phasor estimation has many application areas and has therefore attracted significant research focus. Classical phasor estimation proposed many years ago, considers the phasor to be time independent which means constant amplitude and phase. However, the dynamic phasor concept introduced recently, improves the accuracy of the phasor estimation under a non-stationary signal as is typically the case of low frequency oscillations (LFO). However, more accurate estimates lead to higher computation time. To achieve both low computation time and more accurate estimates, an adaptive phasor estimation concept based on both static and dynamic phasors is proposed in this paper. A new method based on the *Adaptive Prony* algorithm is presented, in which the *Static Prony* is employed under steady state conditions and the *Dynamic Prony* under dynamic conditions. To switch between these two algorithms, a Cumulative Summation of the Phasor Estimation Error ($CSPEE$) is used. Simulation results show the applicability of the proposed method to achieve the most accurate estimates at the lowest computation time. Total Vector Error (TVE) and Floating Point Operation ($FLOP$) are used to evaluate the proposed method.**

I. Introduction

A dynamic phasor is a complex envelope of a sinusoidal signal with variable amplitude and phase. It plays an increasingly important role in the analysis of power systems under non-steady state conditions. Power systems may operate close to their stability limits where a disturbance can bring them to a state characterized by low frequency oscillations (LFO). The LFO is a phenomenon of large fluctuations in active and reactive power flows between two areas of the power system, resulting from severe disturbances like line faults, loss of generating units or switching of heavy loads [1], [2]. In the literature, a number of alternative analytical methods are proposed to estimate the dynamic phasor [3]. In [4], a new method based on an adaptive band-pass filter was proposed while [5] introduced an angle-shifted energy operator to extract the instantaneous amplitude. An integrated phasor and frequency estimation using a fast recursive GaussNewton algorithm was proposed in [6] and a method based on modified Fourier Transform was presented in [7] to eliminate the DC offset. A PLL-Taylor-Fourier method is proposed in [8]to improve the accuracy of the estimates by using a Phase Lock Loop (PLL) under off-nominal frequency conditions. A phasor estimation algorithm based on the least square curve fitting was proposed in [9] to overcome the CT saturation effect. In [10], an approach based on a recursive wavelet transform was introduced to estimate the phasor parameters. In [11] the phasor and frequency measurements under transient system conditions were discussed. Maximally Flat Differentiators (MFD) [12] and phasorlet [13] are also two other methods for dynamic phasor estimation. The Taylor Fourier algorithm proposed in [14] approximates the dynamic phasor using the second-order Taylor Expansion and least square observer. A Taylor Kalman method was used in [15] as a Kalman observer to estimate the dynamic phasor without delay and was enhanced in [16] by developing the state space under harmonic conditions. The Shank method is another dynamic phasor estimation algorithm that employs the least square and consecutive delays of the unit response [17].

The Prony algorithm approximates the main signal by exponentially damped sinusoidal signals. It is able to determine the values of frequency, damping factor, amplitude and phase of the main signal. Frequency and damping factor are calculated in the first step and then the amplitude and phase are obtained in the second step [18]. The *Dynamic Prony* based on the second order Taylor expansion is proposed in [18], [19] and compared with the classical Prony that estimates the static phasor. It was shown that the accuracy of a dynamic phasor is higher than a static phasor during LFO. However, the computational burden of the dynamic phasor is larger since there are more terms in the Taylor expansion. This fact is the motivation for proposing an adaptive approach for the phasor estimation to provide an accurate and fast algorithm. The accuracy of the phasor estimation based on the static phasor concept is as accurate as the dynamic concept under the steady state conditions. On the other hand, LFO resulting from a dynamic condition is a transient phenomenon in a power system. Therefore, it is proposed to employ the static phasor under steady state and the dynamic phasor under the LFO conditions. To switch between the two concepts (static or dynamic), an index based on Cumulative Summation of the Phasor Estimation Error ($CSPEE$) is used. To summarize, the main contribution of this paper is to propose an adaptive concept for phasor estimation which may be employed to other algorithms to make them more efficient.

This work was supported by ERCIM.

978-1-5386-5326-5/18/$31.00 ©2018 IEEE

II. Phasor Estimation based on *Prony*

Consider a general sinusoidal quantity given by:

$$s(t) = a(t)e^{\alpha t} cos(2\pi f_1 t + \phi(t)) \quad (1)$$

where $a(t)$ and $\phi(t)$ are the amplitude and phase angle of the main signal $s(t)$. f_1 is the fundamental frequency and α is the damping factor. $p(t)$ is the phasor (complex envelope) defined:

$$p(t) = a(t)e^{j\phi(t)} \quad (2)$$

By substituting (2) in (1), $s(t)$ can be written as:

$$s(t) = \frac{1}{2}(p(t)e^{(\alpha+j2\pi f_1)t} + p(t)^* e^{(\alpha-j2\pi f_1 t)}) \quad (3)$$

The Taylor series of $p(t)$ at $t = 0$ is:

$$p(t) = p_0 + p_1 t + p_2 t^2 + ... + p_k t^k \quad (4)$$

$$p_0 = p(t=0), p_1 = \frac{dp}{dt}(t=0), ..., p_k = \frac{1}{k!}\frac{d^k p}{dt^k}(t=0)$$

where the coefficients of the series $(p_0, p_1, p_2, , p_k)$ are derivatives of the phasor at the observation center. Based on the number of Taylor coefficients, the two different Prony algorithms are: the *Static Prony* and the *Dynamic Prony*. Detailed descriptions of these methods are given in [18], [19]. *Static Prony* is used as an alternative name for the zeroth-order Taylor Prony while the *Dynamic Prony* is similar for the second-order Taylor Prony.

A. Static Prony

The *Static Prony* is based on just the first component of the Taylor expansion (zeroth-order Taylor series) presented in (4). The estimated phasor by the *Static Prony* is called the static phasor. According to the zeroth-order Taylor polynomial of $p(t)$ we have:

$$s(t) = \frac{1}{2}(p_0.e^{(\alpha+j2\pi f_1)t} + p_0^* e^{(\alpha-j2\pi f_1)t}) \quad (5)$$

With N samples of $s(t)$ we have:

$$\begin{pmatrix} s[0] \\ \vdots \\ s[n] \\ \vdots \\ s[N-1] \end{pmatrix} = \frac{1}{2} \begin{pmatrix} 1 & 1 \\ \vdots & \vdots \\ Z_1^n & {Z_1}^{-n} \\ \vdots & \vdots \\ Z_1^{(N-1)} & {Z_1}^{-(N-1)} \end{pmatrix} \begin{pmatrix} p_0 \\ p_0^* \end{pmatrix} \quad (6)$$

$$\boldsymbol{S} = \boldsymbol{J}^{(0)} \ \boldsymbol{P}^{(0)}$$

where $Z_1 = e^{(\alpha+j2\pi f_1)T}$ and T is the sampling period. The best estimate of the static phasor is (tr is the transpose operator):

$$\boldsymbol{P}^{(0)}_{estimated} = (\boldsymbol{J}^{(0)^{tr}} \boldsymbol{J}^{(0)})^{-1} \boldsymbol{J}^{(0)^{tr}} \boldsymbol{S} \quad (7)$$

The static phasor, estimated by the zeroth-order Taylor series, is a time invariant parameter. In other words, the phasor is modeled as a constant amplitude and phase quantity in the estimation process. Therefore, this model fits the stationary signal measured under steady state conditions. Accordingly, the estimated phasor by the *Static Prony* is the most accurate estimate under the steady state conditions.

B. Dynamic Prony

A phasor with time varying amplitude and phase is a more accurate representation under dynamic conditions of a power system as during Low Frequency Oscillations (LFO). Therefore, the dynamic phasor concept is modelled using a second-order Taylor series expansion. According to the second-order Taylor polynomial of $p(t)$, we have:

$$s(t) = \frac{1}{2}([p_0 + p_1 t + p_2 t^2].e^{(\alpha+j2\pi f_1)t} + [p_0^* + p_1^* t + p_2^* t^2]e^{(\alpha-j2\pi f_1)t}) \quad (8)$$

Presume that the signal $s(t)$ is sampled by N samples per cycle, and can be expressed as:

$$\boldsymbol{S} = \boldsymbol{J}^{(2)} \ \boldsymbol{P}^{(2)} \quad (9)$$

where its detailed representation ($N' = N - 1$) is shown at the end of this page. The best estimate of the dynamic phasor, is obtained as:

$$\boldsymbol{P}^{(2)}_{estimated} = (\boldsymbol{J}^{(2)^{tr}} \boldsymbol{J}^{(2)})^{-1} \boldsymbol{J}^{(2)^{tr}} \boldsymbol{S} \quad (10)$$

The second order of the Taylor series helps to estimate the time varying phasor under the non-stationary conditions and therefore improves the accuracy of the phasor estimates. This was the major difference between the *Static Prony* and *Dynamic Prony*, except for these both algorithms are similar. According to (6) or (9), the phasor is estimated based on the root Z_1 extracted from the roots of the characteristic equation. This equation is in terms of the new parameters (a_0, a_1 and a_2) defined as:

$$F(z) = (z - Z_1)(z - Z_1^*) = a_0 z^2 + a_1 z + a_2 \quad (11)$$

$$\begin{pmatrix} s[0] \\ \vdots \\ s[n] \\ \vdots \\ s[N'] \end{pmatrix} = 0.5 \begin{pmatrix} 0 & 0 & 1 & 1 & 0 & 0 \\ \vdots & \vdots & \vdots & \vdots & \vdots & \vdots \\ (nT)^2 Z_1^n & (nT)Z_1^n & Z_1^n & Z_1^{*n} & (nT)Z_1^{*n} & (nT)^2 Z_1^{*n} \\ \vdots & \vdots & \vdots & \vdots & \vdots & \vdots \\ ((N')T)^2 Z_1^{(N')} & ((N')T)Z_1^{(N')} & Z_1^{(N')} & Z_1^{*(N')} & ((N')T)Z_1^{*(N')} & ((N')T)^2 Z_1^{*(N')} \end{pmatrix} \begin{pmatrix} p_2 \\ p_1 \\ p_0 \\ p_0^* \\ p_1^* \\ p_2^* \end{pmatrix}$$

The coefficients of characteristic equation are found from:

$$\begin{pmatrix} s[0] \\ s[1] \\ s[2] \\ \vdots \\ s[N-1] \end{pmatrix} = \begin{pmatrix} s[-1] & s[-2] & s[-3] \\ s[0] & s[-1] & s[-2] \\ s[1] & s[0] & s[-1] \\ \vdots & \vdots & \vdots \\ s[N-2] & s[N-3] & s[N-4] \end{pmatrix} \begin{pmatrix} a_0 \\ a_1 \\ a_2 \end{pmatrix}$$

$$\boldsymbol{S} = \boldsymbol{Q}\ \boldsymbol{a} \tag{12}$$

$$\boldsymbol{a} = (\boldsymbol{Q}^{tr}\boldsymbol{Q})^{-1}\boldsymbol{Q}^{tr}\boldsymbol{S} \tag{13}$$

III. Adaptive Prony (Proposed method)

According to the previous section, the static phasor is a suitable representation under the steady state conditions. However, in non-stationary conditions as for example under low frequency oscillations (LFO), the amplitude and phase are time varying and require dynamic representations. Although the accuracy of the *Dynamic Prony* is better than the *Static Prony*, the computational burden of the dynamic phasor is larger. According to the inherent characteristic of the LFO (being temporary), an adaptive strategy is proposed in this section to switch between the static and dynamic phasor concepts during the phasor estimation. Therefore, the *Static Prony* is used under the steady state conditions and the *Dynamic Prony* under the dynamic conditions. To switch between these concepts, the proposed index in [20], Cumulative Summation of the Phasor Estimation Error($CSPPE$), is used as:

$$t(n) = s(n) - s_{est}(n), \quad CSPEE(n) = \sum_{n=r-N}^{r} |t(n)| \tag{14}$$

where $s(n)$ is the main signal, $s_{est}(n)$ is the recomputed signal using the estimated phasor while the phasor estimation error $t(n)$ is the difference between them. The $CSPEE(n)$ is calculated by cumulative summation of the $t(n)$ over one cycle. The concept of the adaptive phasor estimation is shown in Fig.1. Firstly, the estimation process is started by the *Static Prony* and the $CSPEE$ is monitored continuously. If the $CSPEE$ is lower than a threshold value (TR), the signal is under stationary conditions and the *Static Prony* is continued to deliver the most accurate estimate. Once the LFO starts, the amplitude and phase fluctuate and when $CSPEE$ increases beyond the threshold, the *Dynamic Prony* is replaced with the *Static Prony*. Hence the adaptive strategy provides the most accurate estimate using the least computational effort.

IV. Adaptive phasor concept with Least square and Kalman Filter

The adaptive phasor concept presented in the previous section, is a general concept that can be employed to any other phasor estimation algorithm. In this section, this concept is employed to the Least square and the Kalman filter. The Taylor-least-square and Taylor-Kalman-filter are made adaptive in this section. Detailed descriptions of these methods are presented in [14] and [15]. *Static least square* means that the zeroth-order Taylor Fourier is used under steady state conditions while the *Dynamic least square* means that the second-order Taylor Fourier is used under dynamic conditions. Finally, adaptive least square means a combination of two mentioned methods using an adaptive procedure. The same explanation can be done for the Kalman method.

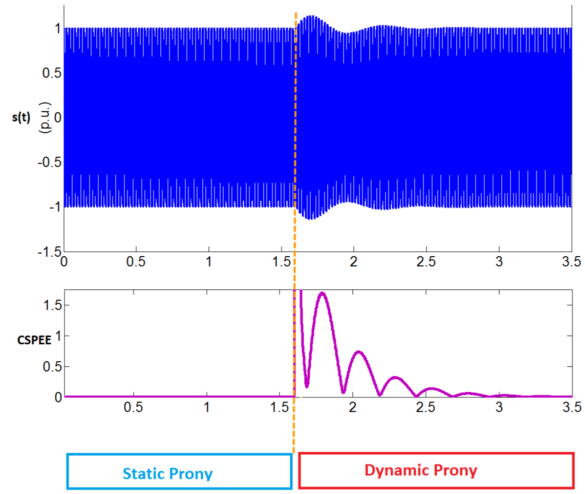

Fig. 1. Concept of adaptive phasor estimation

A. Adaptive least square (zeroth-order Taylor Fourier under steady state conditions and second-order Taylor Fourier under dynamic conditions)

The least square algorithm uses a data window where an old sample is removed when a new measured sample is inserted into the window. Although the use of a window makes it powerful in the transient periods, the window creates a delay as long as the window length. The adaptive least square proposed here is based on a switching between the static least square (zeroth-order Taylor least square) and the dynamic least square (second-order Taylor least square) by monitoring the $CSPEE$. According to (3) and (4), the adaptive least square switches between equations (15) and (16). Details are given at the end of next page.

$$\begin{pmatrix} s(0) \\ \vdots \\ s(N_h) \\ \vdots \\ s(N-1) \end{pmatrix} = \frac{1}{2} \begin{pmatrix} e^{-j.N_h.\omega_1} & e^{+j.N_h.\omega_1} \\ \vdots & \vdots \\ 1 & 1 \\ \vdots & \vdots \\ e^{+j.N_h.\omega_1} & e^{-j.N_h.\omega_1} \end{pmatrix} \begin{pmatrix} p_0 \\ p_0^* \end{pmatrix} \tag{15}$$

where $\omega_1 = 2\pi/N$ and N_h is the middle sample in the data window.

B. Adaptive Kalman (zeroth-order Kalman under steady state and second-order Kalman under dynamic conditions)

Kalman filter is an powerful method to compute the state variables recursively and instantaneously. Contrary to the least square, the Kalman filter is based on a state space model. The state space is a complete model for analyzing a dynamic system. In this model, the state value at each sample is calculated from its previous value. The main advantage of the Kalman filter is the property of instantaneous tracking. The adaptive Kalman proposed in this paper is based on a switching between the static Kalman (zeroth-order Taylor Kalman) and the dynamic Kalman (second-order Taylor Kalman) by monitoring the $CSPEE$. According to the derivatives of the $p(t)$, the adaptive Kalman switches between state transition matrices (17) and (18).

$$\varphi^{(0)} = \begin{pmatrix} e^{j\theta_1} & 0 \\ 0 & e^{-j\theta_1} \end{pmatrix} \tag{17}$$

$$\varphi^{(2)} = \begin{pmatrix} e^{j\theta_1} & \tau e^{j\theta_1} & \frac{\tau^2}{2!}e^{j\theta_1} & 0 & 0 & 0 \\ 0 & e^{j\theta_1} & \tau e^{j\theta_1} & 0 & 0 & 0 \\ 0 & 0 & e^{j\theta_1} & 0 & 0 & 0 \\ 0 & 0 & 0 & e^{-j\theta_1} & \tau e^{-j\theta_1} & \frac{\tau^2}{2!}e^{-j\theta_1} \\ 0 & 0 & 0 & 0 & e^{-j\theta_1} & \tau e^{-j\theta_1} \\ 0 & 0 & 0 & 0 & 0 & e^{-j\theta_1} \end{pmatrix} \tag{18}$$

where $\theta_1 = 2\pi/N$ and τ is the sampling time. Since the Kalman filter is an instantaneous estimator, switching between the two state transition matrices creates a transient behavior during the switching time. To overcome this problem, an overlap concept is proposed. When the $CSPEE$ increases, the dynamic Kalman should be replaced with the static Kalman. However, an overlap time is anticipated in the proposed method to allow the Kalman gain to freeze to a new value. The overlap prevents the considerable transient behaviour in the estimates. However, the adaptive least square and the *Adaptive Prony* do not need this strategy since they are data-window-based algorithms.

V. Simulation Results

The simulation results are organized in three subsections where the first is to evaluate the performance of the *Adaptive Prony* with a synthesized signal. The second is about the adaptive least square and the adaptive Kalman with a synthesized signal, while the last shows the performance of the *Adaptive Prony* with a measured signal from a three-machine system.

A. Adaptive Prony with synthesized signal

This subsection includes two parts. The first one is about undamped LFO and the second one is about damped LFO.

1) Undamped LFO: Consider the test case as:

$$S(t) = a(t)\ cos(2\pi f_1 t + \phi(t)) \tag{19}$$

$$\begin{array}{ll} a(t) = 1, \phi(t) = 0 & 0 < t < 1.6s \\ a(t) = 1 + (0.2sin(4\pi t)), \phi(t) = 0 & 1.6 < t < 3s \end{array}$$

The main signal is sampled at $5kHz$ and there are 100 samples per window. $f_1 = 50Hz$ is the fundamental frequency. The signal is stationary in between $0 < t < 1.6$ seconds and non-stationary after $t = 1.6$ seconds (undamped LFO with frequency $2Hz$). The *Adaptive Prony* is used and the results are shown in Fig.2. In Fig.2, the top subfigure is the main signal, the middle subfigure is the real and estimated amplitude and the last subfigure is the switch action that shows the switching times between the static phasor (is numbered as ”1”) to the dynamic phasor (is numbered as ”2”). According to the Fig.2, *Adaptive Prony* estimates the static phasor before $t = 1.6$ seconds and the dynamic phasor after $t = 1.6$ seconds. This adaptive strategy is implemented by monitoring the $CSPEE$. Since the signal is under stationary conditions before $t = 1.6$ seconds, the static phasor delivers the most accurate estimate at lowest computational cost. This condition is detected by monitoring the $CSPEE$ and comparing with a threshold (1×10^{-5}). The threshold is selected based on analyzing many cases and obtaining maximum value of the $CSPEE$ during LFO. After $t = 1.6$ seconds, the $CSPEE$ increases and when it is higher than the threshold, the dynamic phasor is activated.

2) Damped LFO: Consider the test case as:

$$S(t) = a(t)\ cos(2\pi f_1 t + \phi(t)) \tag{20}$$

$$\begin{array}{ll} a(t) = 1, \phi(t) = 0 & 0 < t < 1.6 \\ a(t) = 1 + (0.2sin(4\pi t))e^{-t/0.3}, \phi(t) = 0 & 1.6 < t < 6 \end{array}$$

The main signal is stationary in between $0 < t < 1.6$ seconds and the damped LFO is started at $t = 1.6$ seconds. The main signal, the estimated amplitude by *Adaptive Prony* and the switch action are shown in Fig.3. Similarly to the previous subsection, the *Adaptive Prony* estimates the phasor by the static concept before $t = 1.6$ seconds. As a result of the LFO, the $CSPEE$ increases and the dynamic concept is replacing the static. When the $CSPEE$ becomes smaller than the threshold (1×10^{-5}), the static concept is triggered again.

$$\begin{pmatrix} S(0) \\ \vdots \\ S(N_h) \\ \vdots \\ S(N-1) \end{pmatrix} = \frac{1}{2} \begin{pmatrix} N_h^2 e^{-j.N_h.\omega_1} & -N_h e^{-j.N_h.\omega_1} & e^{-j.N_h.\omega_1} & e^{+j.N_h.\omega_1} & -N_h e^{+j.N_h.\omega_1} & N_h^2 e^{+j.N_h.\omega_1} \\ \vdots & \vdots & \vdots & \vdots & \vdots & \vdots \\ 0 & 0 & 1 & 1 & 0 & 0 \\ \vdots & \vdots & \vdots & \vdots & \vdots & \vdots \\ N_h^2 e^{j.N_h.\omega_1} & N_h e^{j.N_h.\omega_1} & e^{j.N_h.\omega_1} & e^{-j.N_h.\omega_1} & N_h e^{-j.N_h.\omega_1} & N_h^2 e^{-j.N_h.\omega_1} \end{pmatrix} \begin{pmatrix} p_2 \\ p_1 \\ p_0 \\ p_0^* \\ p_1^* \\ p_2^* \end{pmatrix} \tag{16}$$

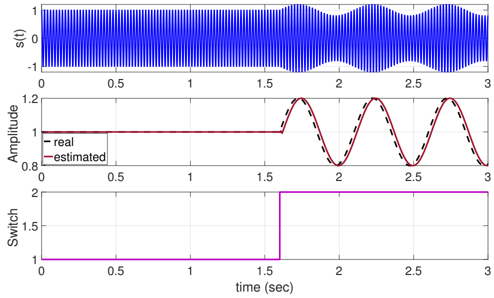

Fig. 2. Adaptive Prony with undamped LFO

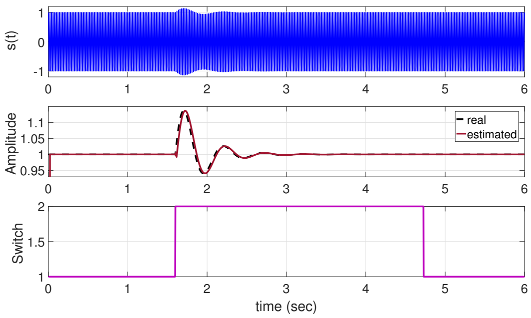

Fig. 3. Adaptive Prony with damped LFO

B. Adaptive Least square and adaptive Kalman Filter

In this section, the simulation results of the adaptive least square and adaptive Kalman filter are presented. These two methods are examined both in undamped and damped LFO.

1) Undamped LFO: To examine the performance of the adaptive least square and adaptive Kalman, undamped LFO presented in (20) is used. Adaptive least square uses the static concept of phasor before $t = 1.6s$ and the dynamic concept of phasor after $t = 1.6s$. Additionally, the adaptive Kalman uses the static state transition matrix during $0 < t < 1.6s$ and the dynamic state transition matrix during $1.6s < t < 3s$. To compare all the six methods, Total Vector Error ($TVE = |p_r - p_e|/|p_r|$, where p_r is the real phasor and p_e is the estimated phasor) index and number of Floating Points (FLOPs) are tabulated in Table III. According the table, the accuracy of the dynamic phasor is higher than the static phasor while the computational burden (FLOPs) of the static phasor is lower. However, the proposed adaptive phasor is accurate and its computational burden is efficient ('-' is put in table because it depends on which concept that is used in the adaptive method). For example, for calculating 100 samples of one cycle by adaptive Kalman, the number of FLOPs is $(50 \times 130) + (50 \times 1436)$.

2) Damped LFO: Consider the test case presented in (20). Similar to the previous subsection, adaptive least square estimates the static phasor during the stationary condition and the dynamic phasor during non-stationary condition. The same strategy is also employed for the adaptive Kalman and the results are tabulated in Table IV. According to table IV, the adaptive strategy provides both suitable accuracy and efficient computational burden.

TABLE I
LEAST SQUARE AND KALMAN WITH UNDAMPED LFO

ine Method	TVE (%)	FlOPs per sample
Static least square	0.1495	4042
Dynamic least square	0.0228	31799
Adaptive least square	0.0228	-
Static Kalman	0.1629	130
Dynamic Kalman	0.0227	1436
Adaptive Kalman	0.0227	-

TABLE II
LEAST SQUARE AND KALMAN WITH DAMPED LFO

Method	TVE (%)	FlOPs per sample
Static least square	0.0240	4042
Dynamic least square	0.0067	31799
Adaptive least square	0.0067	-
Static Kalman	0.0245	130
Dynamic Kalman	0.0071	1436
Adaptive Kalman	0.0071	-

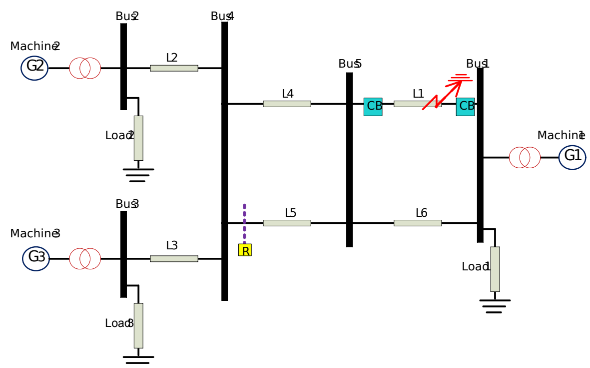

Fig. 4. Three-machine power system

C. Adaptive Prony in a three-machine power system

To examine the proposed *Adaptive Prony* in a more realistic setting, a three-machine power system shown in Fig.4 is modeled and simulated using SIMULINK [21]. Fundamental frequency is $60Hz$ and there are 512 samples per cycle. A three-phase fault is simulated at 90% of the line connecting bus 5 and bus 1. The fault occurs at $t = 1$ second and is cleared after 0.03 seconds. This event causes a LFO and is observed by a distance relay (R) at transmission line L_5.

The measured current (Fig.5) is under stationary condition in between $0 < t < 1$ seconds and then low frequency oscillation is started after $t = 1$ second. The measured current by the distance relay, the estimated amplitude by the *Adaptive Prony* and the switching action are shown in Fig.5. The *Adaptive Prony* estimates phasor by the static concept (is numbered as '1' in the bottom subfigure of Fig.5) from $t = 0$ till $t = 1.0$ seconds. Then $CSPEE$ increases and the proposed method triggers the *Dynamic Prony* (is numbered as '2').

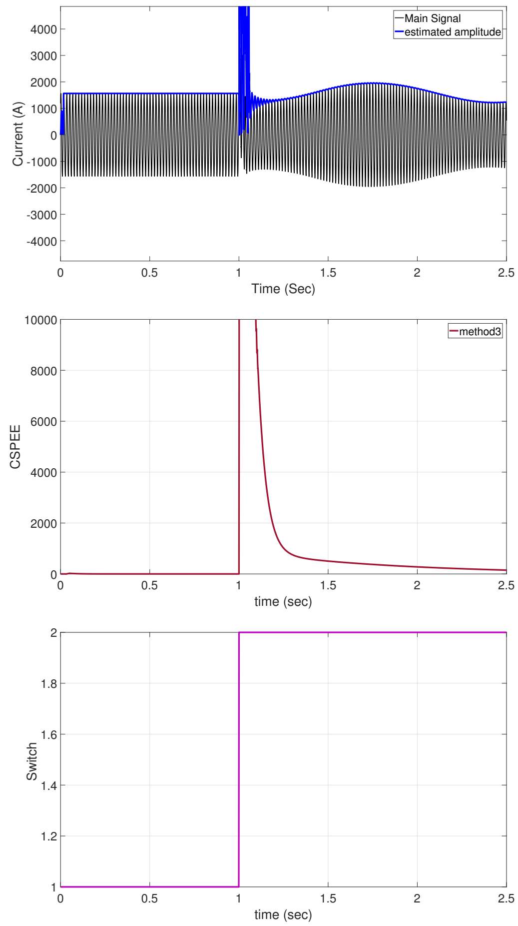

Fig. 5. Adaptive Prony with measured signal in three-machine power system

VI. Conclusion

The assumption of constant amplitude and phase in the phasor estimation procedure, imposes strong restrictions on the monitoring and control of power systems. Therefore, the concept of dynamic phasors has attracted significant attention. However, it is demonstrated that the dynamic phasor estimation methods increase the computational burden. It is therefore a trade-off between reduced accuracy of the static phasor estimation methods compared to higher computational cost of the dynamic approaches for non-stationary signals appearing for example from Low Frequency Oscillations. In this paper, it is shown that an adaptive strategy of phasor estimation is more appropriate. An index named Cumulative Summation of Phasor Estimation Error ($CSPEE$) is used to detect the change in accuracy of the phasor estimate for employing the adaptive strategy. According to the proposed method, $CSPEE$ is monitored continuously and the appropriate method of each condition (static or dynamic) is adopted based on the value of $CSPEE$. The static version of the phasor estimation algorithms is used under static conditions and the dynamic version is used under dynamic conditions. Simulation results reveal the capabilities of the proposed method to reduce the computational burden while keeping an acceptable accuracy under different conditions. As a future research direction, an effective strategy for time-varying sampling would further improve the efficiency of the phasor estimation algorithms.

References

[1] N. Kumar, "Comparison of power system stabiliser with series and shunt facts controllers in damping power system oscillations," *Australian Journal of Electrical and Electronics Engineering*, vol. 7, no. 1, pp. 1–14, 2010.

[2] M. H. Haque, "Use of sssc to improve first swing stability limit and damping of a power system," *Australian Journal of Electrical and Electronics Engineering*, vol. 3, no. 1, pp. 17–26, 2006.

[3] Y.-J. Kwon and S.-T. Kim, "Modified dynamic phasor estimation method during a transient period," *Journal of International Council on Electrical Engineering*, vol. 1, no. 2, pp. 175–180, 2011.

[4] I. Kamwa, A. K. Pradhan, and G. Joos, "Adaptive phasor and frequency-tracking schemes for wide-area protection and control," *IEEE Transactions on Power Delivery*, vol. 26, no. 2, pp. 744–753, 2011.

[5] X. Jin, F. Wang, and Z. Wang, "A dynamic phasor estimation algorithm based on angle-shifted energy operator," *Science China Technological Sciences*, vol. 56, no. 6, pp. 1322–1329, 2013.

[6] P. Dash, K. Krishnanand, and R. Patnaik, "Dynamic phasor and frequency estimation of time-varying power system signals," *International Journal of Electrical Power & Energy Systems*, vol. 44, no. 1, pp. 971–980, 2013.

[7] S.-H. Kang, D.-G. Lee, S.-R. Nam, P. A. Crossley, and Y.-C. Kang, "Fourier transform-based modified phasor estimation method immune to the effect of the dc offsets," *IEEE Transactions on Power Delivery*, vol. 24, no. 3, pp. 1104–1111, 2009.

[8] J. A. de la O Serna, "Synchrophasor measurement with polynomial phase-locked-loop taylor–fourier filters," *IEEE Transactions on Instrumentation and Measurement*, vol. 64, no. 2, pp. 328–337, 2015.

[9] D.-G. Lee, S.-H. Kang, and S.-R. Nam, "Phasor estimation algorithm based on the least square technique during ct saturation," *Journal of Electrical Engineering and Technology*, vol. 6, no. 4, pp. 459–465, 2011.

[10] A. G. Phadke and B. Kasztenny, "Synchronized phasor and frequency measurement under transient conditions," *IEEE Transactions on Power Delivery*, vol. 24, no. 1, pp. 89–95, 2009.

[11] J. Ren and M. Kezunovic, "Real-time power system frequency and phasors estimation using recursive wavelet transform," *IEEE Transactions on Power Delivery*, vol. 26, no. 3, pp. 1392–1402, 2011.

[12] M. A. Platas-Garza, J. Platas-Garza, and J. A. de la O Serna, "Dynamic phasor and frequency estimates through maximally flat differentiators," *IEEE Transactions on Instrumentation and Measurement*, vol. 59, no. 7, pp. 1803–1811, 2010.

[13] J. A. O. Serna, "Phasor estimation from phasorlets," *IEEE transactions on instrumentation and measurement*, vol. 54, no. 1, pp. 134–143, 2005.

[14] J. A. de la O Serna, "Dynamic phasor estimates for power system oscillations," *IEEE Transactions on Instrumentation and Measurement*, vol. 56, no. 5, pp. 1648–1657, 2007.

[15] J. A. de la O Serna and J. Rodriguez-Maldonado, "Instantaneous oscillating phasor estimates with taylor-kalman filters," *IEEE Transactions on Power Systems*, vol. 26, no. 4, pp. 2336–2344, 2011.

[16] J. A. De la O Serna and J. Rodríguez-Maldonado, "Taylor–kalman–fourier filters for instantaneous oscillating phasor and harmonic estimates," *IEEE Transactions on Instrumentation and Measurement*, vol. 61, no. 4, pp. 941–951, 2012.

[17] A. T. Muoz and J. A. de la O Serna, "Shanks' method for dynamic phasor estimation," *IEEE Transactions on Instrumentation and Measurement*, vol. 57, no. 4, pp. 813–819, 2008.

[18] J. Khodaparast and M. Khederzadeh, "Dynamic synchrophasor estimation by taylor–prony method in harmonic and non-harmonic conditions," *IET Generation, Transmission & Distribution*, 2017.

[19] J. A. de la O Serna, "Synchrophasor estimation using prony's method," *IEEE Transactions on Instrumentation and Measurement*, vol. 62, no. 8, pp. 2119–2128, 2013.

[20] A. G. Phadke and J. S. Thorp, *Synchronized phasor measurements and their applications*. Springer, 2008, vol. 1.

[21] J. Khodaparast and MKhederzadeh, "Modified concentric power swing blocker applicable in upfc compensated line," *IET Generation, Transmission & Distribution*, 2017.